Chinese Chemical Letters 32 (2021) 525–528

Contents lists available at ScienceDirect

Chinese Chemical Letters

journal homepage: www.elsevier.com/locate/cclet

Communication

Solvent induced enhancement of nonlinear optical response of graphdiyne

Yuze Dong[a,b], Sergey Semin[b], Yaqing Feng[a,d,*], Jialiang Xu[a,c,**], Theo Rasing[b]

[a] School of Chemical Engineering and Technology, Tianjin University, Tianjin 300350, China
[b] Radboud University, Institute for Molecules and Materials (IMM), Heyendaalseweg 135, 6525AJ, Nijmegen, the Netherlands
[c] School of Materials Science and Engineering, Nankai University, Tianjin 300350, China
[d] Collaborative Innovation Center of Chemical Science and Engineering (Tianjin), Tianjin University, Tianjin 300072, China

ARTICLE INFO

Article history:
Received 13 February 2020
Received in revised form 30 March 2020
Accepted 31 March 2020
Available online 18 April 2020

Keywords:
2D materials
Graphdiyne
Nonlinear optics
Kerr-effect
Solvent effect

ABSTRACT

Flat and crystalline materials with exceptional nonlinear optical (NLO) properties are highly desirable for their potential applications in integrated NLO photonic devices. Graphdiyne (GD), a new two-dimensional (2D) carbon allotrope, has recently evoked burgeoning research attention by virtue of its tunable bandgap along with a high carrier mobility and extended π-conjugation compared with most conventional optical materials. Here, we experimentally probe the third-order nonlinear optical response of GD dispersed in several common solvents (alcohols) using a femtosecond Z-scan technique. The measured nonlinear optical refractive index is in the order of $\sim 10^{-8}$ cm^2/W, which is approximately one order of magnitude higher than that of most 2D materials. In particular, we find that different NLO responses can be observed from GD when dispersed in different solvents, with the strongest NLO response when dispersed in 1-propanol. It is proposed that some intrinsic properties of the solvents, such as the polarity and viscosity, could influence the NLO response of GD materials. Our experimental results confirm the assumptions on the NLO behavior in GD and demonstrate its great potential for future generations of Kerr-effect-based NLO materials and devices.

Photonic data manipulation and processing promises a significant reduction of energy dissipation and increase in speed, all at extreme bandwidths [1]. However, the intrinsically small light-matter interaction requires materials with strong (nonlinear) optical responses to realize integrated on-chip photonic devices [2–4]. Over the past decades, various materials have been intensively explored for nonlinear optical applications [5–9]. 2D materials have recently triggered a lot of interest because of their fascinating electronic and optical properties [10–12], in association with promising applications such as photovoltaics [13] and optoelectronics [14,15]. For example, graphene, well-known for its many unique properties [16,17], also displays broadband optical-limiting properties, and was considered the most promising medium for optoelectronic devices [18,19]. However, the zero-bandgap nature of graphene constrained its applications to some extent [20,21]. For the fabrication and integration of devices, including optical modulators, transistors, and mode lockers, a finite and rather tunable bandgap is necessary. Some other 2D-materials like two-dimensional transition metal dichalcogenides (TMDs) and black phosphorus (BP) appear to be more promising for technology in that respect [10,11].

Graphdiyne, a new 2D carbon allotrope comprising sp- and sp^2-hybridized carbon atoms, is predicted to be one of the most stable allotropes of the carbon family, with superior electrical properties, high π-conjugation and uniformly porous structure, according to theoretical predictions [22–25]. Unlike zero-bandgap graphene, graphdiyne is an n-type semiconductor with a direct intrinsic bandgap, the value of which has been predicted to be in the range from 0.46 eV to 1.22 eV, based on different calculation methods [26–28]. This would make the bandgap of GD to bridge the gap between the zero-bandgap graphene and the large bandgap (higher than 1.57 eV) semiconducting TMDs for a new generation optoelectronics [29]. Most importantly, the existence of acetylenic bonds offer innovative approaches for structure flexibility as well as property modification, making it favorable for wider applications compared with conventional 2D materials [24,25]. Since the first synthesis of GD by Li's group [22], the potential of this unique

* Corresponding author at: School of Chemical Engineering and Technology, Tianjin University, Tianjin 300350, China.
** Corresponding author at: School of Materials Science and Engineering, Nankai University, Tianjin 300350, China.
E-mail addresses: yqfeng@tju.edu.cn (Y. Feng), jialiang.xu@nankai.edu.cn (J. Xu).

https://doi.org/10.1016/j.cclet.2020.03.078
1001-8417/

material was shown in solar cells [30,31], lithium-ion storage [32,33], electronic devices [34], catalysis [35,36] and beyond. Additionally, GD would, in principle, be an appealing NLO material on account of its large π-conjugation system and direct bandgap [37]. However, research of the nonlinear optical properties of GD remains relatively scarce [38,39].

In this paper, we report experimental investigations of the third-order nonlinear optical response of GD dispersions using a Z-scan technique. It is found that GD dispersions exhibit a pronounced nonlinear optical self-defocusing effect under femtosecond excitation. The nonlinear refractive index is estimated to be in the order of 10^{-8} cm^2/W, which is much higher than that of most conventional 2D materials. Additionally, the nonlinear refractive index of GD is found to be very different when it is dispersed in various solvents. The polarity of the solvent, in combination with its viscosity, is proposed to greatly influence the NLO response of GD. Our experiments clearly validate that GD nanostructures are effective NLO candidates for Kerr-effect-based NLO applications.

To obtain the GD film, it is an essential part to synthesize the hexaethynylbenzene (HEB) monomer, which was prepared from the deprotection of its precursor hexakis[(trimethylsilyl)ethynyl] benzene (HEB-TMS) [40]. Typically, HEB-TMS (4 mg) was dissolved in 60 mL of degassed dichloromethane with 0.1 mL of tetrabutylammonium fluoride as the deprotection agent. The reaction mixture was continuously stirred for 10 min under an argon atmosphere in the dark. The obtained solution was used for the next synthetic process immediately without any further purification steps.

The GD films were synthesized *via* a liquid/liquid interfacial method according to the literature [41]. Briefly, 10 mL of the solution of HEB in dichloromethane (0.1 mmol/L) was added to a glass cylinder, and the upper liquid layer was covered with 10 mL of dual water. Then, 10 mL of aqueous solution of copper acetate (0.01 mol/L) containing 0.25 mol/L of pyridine was dropped slowly to the aqueous phase to form two separate phases. The entire process was carried out at room temperature under argon atmosphere. The system was kept vibration-free for >24 h, and a brown thin film was formed at the interface between the liquids. The top layer liquid was substituted with aqueous HCl solution (1 mol/L) and deionized water, successively, while the bottom layer was replaced with degassed dichloromethane. The obtained films were then dispersed in alcohol solvents for further characterization. Additionally, with the aid of sonication for about 1 h at room temperature, GD nanofilms were dispersed in different common solvents, including methanol (MeOH), ethanol (EtOH), 1-propanol (1-PrOH) and *n*-butanol (*n*-BuOH). The resulting suspensions were mildly centrifugated to remove any lager flakes, and in this way homogeneous and stable dispersions of GD film in these solvents are obtained for optical measurements.

The morphology of the GD films was studied by TEM (Fig. 1a), verifying that the films obtained at the liquid/liquid interface are flat and continuous. The HRTEM image revealed a layer-by-layer structure of the films with an interval of 0.45 nm (Fig. 1b), consistent with the lattice reported for GD [41,42]. The corresponding SAED patterns showed a hexagonal symmetry, indicating the high crystallinity of the as-prepared GD films.

The elementary composition and structure were characterized by XPS, Raman spectroscopy, XRD and DLS. The successful formation of GD films was essentially confirmed by the high-resolution C 1s XPS spectrum (Fig. 2a). In detail, the peak of C 1s can be de-convoluted into four Gaussian curves, corresponding to C=C (sp^2) at 284.6 eV and C≡C (sp) at 285.2 eV, respectively. The other two peaks, at 286.4 eV and 287.5 eV, are assigned to C−O and C=O, which may result from the adsorption of air in the pores of the networks and the oxidation of some terminal alkyne and defects [41]. Furthermore, Raman spectroscopy gives strong evidence of the successful synthesis of GD as well as its intact structure. As depicted in Fig. 2b, the spectrum of the material shows four distinct peaks. The peaks at 1375 and 1575 cm^{-1} correspond to the breathing vibration of aromatic rings (D band) and the stretching vibration of aromatic rings (G band), respectively [43]. Meanwhile, two bands at 1931 cm^{-1} and 2173 cm^{-1} can also be observed, which are derived from the vibration of the conjugated *diyne* linkage [44]. The XRD data show a broad peak near 23.6° (Fig. S1 in Supporting information), which is in good agreement with the spacing between the carbon layers in TEM [45]. Additionally, the size distributions of GD dispersed in these four solvents are very similar, with the average size between 255∼285 nm (Fig. S2 in Supporting information).

The third-order optical nonlinearity of GD was determined with closed aperture (CA) Z-scan measurements performed at different laser intensities, by using a home-built setup excited by a mode-locked Ti:sapphire oscillator at 800 nm, a pulse duration of ∼100 fs, and a repetition rate of 82 MHz. In these measurements, the transmitted radiation through a sample can be measured as a function of incident intensity, with the sample moving through the lens focus [46]. The configuration of the Z-scan setup used in our work is shown in Fig. S3 (Supporting information). The laser beam emitted from a Coherent femtosecond laser was attenuated and then focused by a lens with focal length of 75 mm, producing a beam radius of around 50 μm at the focal point. A 1 mm quartz cuvette containing the GD dispersions was oriented perpendicularly to the beam axis and moved along the Z-axis by means of a linear motorized stage. The radiation through an on-axis aperture was recorded by a photodetector and a digital lock-in amplifier (SR830, Stanford Research, U. S. A.). CS_2 was chosen to calibrate the setup [47].

Fig. 3 displays the variation of the normalized transmittance as a function of the sample position relative to the focus of the lens (Z = 0) for GD dispersed in 1-PrOH at different incident laser intensities. The measured CA Z-scan results showed a typical peak and valley curve, indicating that the GD dispersion has a prominent

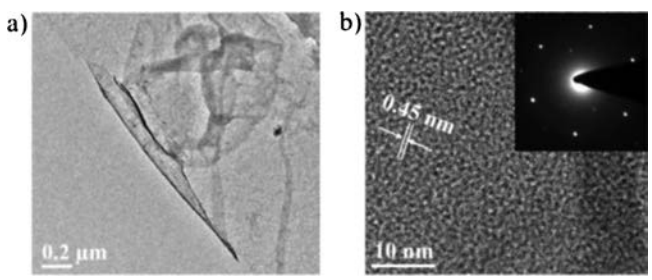

Fig. 1. (a) TEM and (b) HRTEM images of GD film; the inset shows the corresponding SAED pattern.

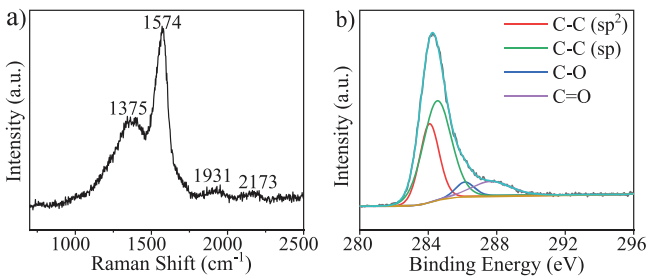

Fig. 2. (a) XPS narrow scan for the element carbon in the GD film on Si(100). (b) Raman spectrum of GD film.

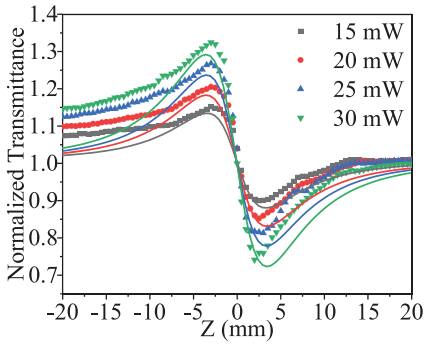

Fig. 3. Experimental results and theoretical fitting for close aperture Z-scan curves of normalized transmittance as a function of sample (GD dispersed in 1-PrOH) position at different incident laser intensities.

self-defocusing effect [48]. The experimental data could be fitted using the following function [46]:

$$T(z) \approx 1 - \frac{4\Delta\Phi\left(\frac{z}{z_0}\right)}{\left(\frac{z_0^2}{z_0^2}+9\right)\left(\frac{z_0^2}{z_0^2}+1\right)} \quad (1)$$

where $T(z)$ is the normalized transmittance, z_0 is the Rayleigh length. $\Delta\Phi$, the on-axis nonlinear phase shift at the focus, is described as $\Delta\Phi_0 = k\, n_2\, I_0\, L_{eff}$, in which k is the wave vector, I_0 is the on-focus intensity and $L_{eff} = L_{cuvette} \times C_{GD}$ is the sample effective thickness, respectively [49].

To negate the effect of the NLO refraction of the solvents, CA Z-scan measurements for pure solvents were also performed under the same conditions (Fig. S4 in Supporting information). The nonlinear phase shift measured within the GD dispersion can be written as $\Delta\Phi_{GD} = \Delta\Phi_{total} - \Delta\Phi_{solvent}$, and the solvent was found to show a small negative nonlinear phase shift (Fig. S4 in Supporting information). Therefore, the n_2 value of GD dispersed in 1-PrOH was caculated to have the value of $\sim 1.1 \times 10^{-8}$ cm^2/W from the aforementioned equation (C_{GD} is taken as 0.1 mg/mL in 1-PrOH). The concentrations of all the GD dispersions were calculated using the Lambert-Beer Law, as displayed in Fig. S5 (Supporting information), together with their linear absorption spectra in the different solvents involved [50]. A linear behavior can be observed for all dispersions with different slopes, which may be attributed to changes in the absorption coefficient owing to differences in dispersion.

GD exhibits the largest NLO refractive effect in intense laser beams (Table 1) compared to other 2D materials [51–54]. It is known that large extended π-conjugation systems, leading to a high molecular hyperpolarizability associated with molecular orientation, can produce a large nonlinearity [55]. GD, possessing a more extended delocalized π-electron framework than graphene, should therefore give rise to a more pronounced NLO refraction. Besides, GD is a direct-narrow-gap semiconductor, the refractive index of which depends significantly on the generation of electron-hole pairs as well as the carrier density. Therefore, the lifetime of electron-hole pairs strongly affects the NLO response.

Table 1
Reported Z-scan results for 2D materials in femtosecond regime.

Sample	Wavelength (nm)	n_2 (cm^2/W)	Reference
Graphdiyne	800	1.1×10^{-8}	Our work
Graphene	1150-2400	1×10^{-9}	[51]
Bi_2Se_3	800	1×10^{-10}	[52]
WS_2	800	8.1×10^{-11}	[53]
Black phosphorus	800	6.8×10^{-11}	[54]

GD has a narrow bandgap with a short recombination lifetime and short response time, resulting in a high nonlinear optical performance [56,57].

Furthermore, for a better insight into the solvent influence on the NLO refractive response, additional experiments were carried out for GD dispersions in various solvents (MeOH, EtOH, 1-PrOH and *n*-BuOH). CA Z-scan measurements for the four GD suspensions were conducted at the same laser intensity (on-axis peak intensities of 0.36 GW/cm^2) and concentration (0.1 mg/mL). We found that the solvents had a remarkable effect on the NLO response of the GD dispersions. As displayed in Fig. 4a, the normalized transmittance curve of GD dispersed in 1-PrOH has the deepest peak and valley, indicating the most prominent NLO performance. The values of the NLO refractive index shown in Fig. 4b were calculated with the same Eq. 1. As can be seen, for similar NLO refractive contributions of the pure solvents, the NLO refractive index value of the 1-PrOH dispersion (1.1×10^{-8} cm^2/W) greatly outperforms those of *n*-BuOH (3.6×10^{-9} cm^2/W), MeOH (1.0×10^{-9} cm^2/W) and EtOH (1.5×10^{-10} cm^2/W) dispersions at the same concentration. That means that the solvent substantially contributes to the obtained NLO refractive indices.

It is known that the NLO refraction is related to physical properties like viscosity and polarity of the solvent [58]. The polarity as well as viscosity of the solvents involved in this work have been listed in Fig. 4c. Here, the viscosities of the solvents are in the order of *n*-BuOH > 1-PrOH > EtOH > MeOH; while the polarities (dielectric constant) follow the trend of MeOH > EtOH > 1-PrOH > *n*-BuOH. As GD is a non-polar molecule, based on the similarity-intermiscibility theory, GD prefers to be dispersed in low-polarity and low-viscosity solvents [59]. Clearly, for the n_2 of GD in four solvents (Fig. 4d), the lower-polarity solvents, such as 1-PrOH and *n*-BuOH, performed better than the higher-polarity solvents, like EtOH and MeOH. However, one exception arises here: 1-PrOH has a higher polarity than *n*-BuOH, but the former presents a better NLO refractive response than the latter, which might be related to the difference in their viscosity.

To rule out the influence of possible aggregation of GD in the various solvents on n_2, its dependence on concentration was determined for different GD dispersions (Fig. S6 in Supporting information). It can clearly be seen that the n_2 of the GD

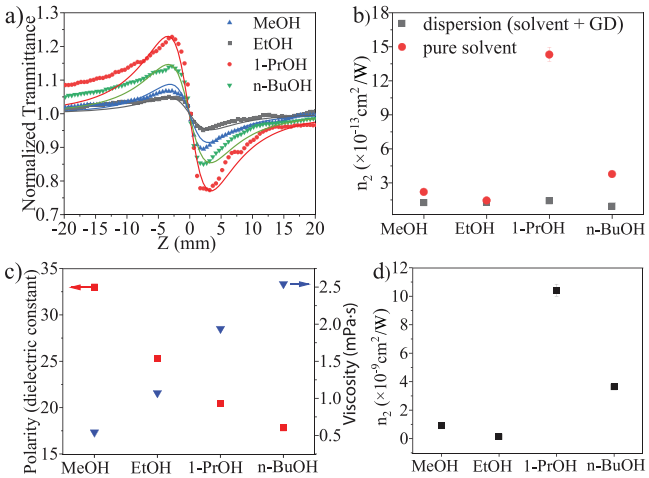

Fig. 4. (a) Experimental results and theoretical fits for close aperture Z-scan curves of normalized transmittance of the GD dispersions in different solvents, with the concentration of the suspension of 0.1 mg/mL, laser power 25 mW at a wavelength of 800 nm and pulse width of 100 fs. (b) Refractive index values of the GD dispersion and relevant pure solvents. (c) Solvent viscosities and dielectric constants for the four solvents at 25 °C [60]. (d) Refractive index values of the GD sample.

dispersions increased almost linearly with increasing concentration, indicating the absence of aggregation of GD.

In summary, we have studied the third-order NLO effect of GD with Z-scan experiments, using 100 fs laser pulses centered at 800 nm on GD dispersed in four different solvents. GD shows a relatively high NLO refraction in the femtosecond regime, surpassing most of known 2D materials. The enhancement is most likely connected to the presence of more extended delocalized π conjugation and the intrinsic bandgap of GD. More interestingly, it is observed that the nonlinear refractive index of 1-PrOH dispersion of GD is better than that of other solvent dispersions employed in our work, which indicates some contributions of the solvent, including the polarity and viscosity, to the improvement of the NLO refraction. Therefore, the presented results open up a path for GD as a promising NLO material for photonic applications, including the influence of the solvent on dispersion for different optical materials. Specifically, GD offers a moderate bandgap of around 0.8 eV, which matches well with the optical communication band (1550 nm, 0.8 eV). Besides, GD has additional advantages as its properties can easily be tailored by chemical derivation or hybridization with other materials in this emerging 2D framework.

Declaration of competing interest

The authors declare that they have no known competing financial interests or personal relationships that could have appeared to influence the work reported in this paper.

Acknowledgments

Financial support from the National Natural Science Foundation of China (Nos. 21773168 and 21761132007) and the Dutch Research Council (NWO) are gratefully acknowledged. Y. Dong is grateful for the supports from the China Scholarship Council (CSC).

Appendix A. Supplementary data

Supplementary material related to this article can be found, in the online version, at doi:https://doi.org/10.1016/j.cclet.2020.03.078.

References

[1] R. Soref, IEEE J. Sel. Top. Quantum Electron. 12 (2006) 1678–1687.
[2] J. Xu, S. Semin, T. Rasing, et al., Small 11 (2015) 1113–1129.
[3] X. Li, S. Semin, L.A. Estrada, et al., Chin. Chem. Lett. 29 (2018) 297–300.
[4] D. Yan, D.G. Evans, Mater. Horiz. 1 (2014) 46–57.
[5] J. Xu, X. Li, J. Xiong, et al., Adv. Mater. (2019) 1806736.
[6] M. Mutailipu, M. Zhang, Z. Yang, et al., Acc. Chem. Res. 52 (2019) 791–801.
[7] B. Lu, S. Liu, D. Yan, Chin. Chem. Lett. 30 (2019) 1908–1922.
[8] D. Yan, H. Yang, Q. Meng, et al., Adv. Funct. Mater. 24 (2014) 587–594.
[9] D. Yan, Chem. Eur. J. 21 (2015) 4880–4896.
[10] X. Duan, C. Wang, A. Pan, et al., Chem. Soc. Rev. 44 (2015) 8859–8876.
[11] Y. Zhou, M. Zhang, Z. Guo, et al., Mater. Horiz. 4 (2017) 997–1019.
[12] Y. Dong, Y. Zhang, X. Li, et al., Small 15 (2019) 1902237.
[13] C. Li, Q. Cao, F. Wang, et al., Chem. Soc. Rev. 47 (2018) 4981–5037.
[14] F. Bonaccorso, Z. Sun, T. Hasan, et al., Nat. Photon. 4 (2010) 611.
[15] Z. Sun, A. Martinez, F. Wang, Nat. Photon. 10 (2016) 227.
[16] A.K. Geim, K.S. Novoselov, The rise of Graphene, Nanoscience and Technology, Macmillan Publishers Ltd., London, 2009, pp. 11–19.
[17] X. Yu, H. Cheng, M. Zhang, et al., Nat. Rev. Mater. 2 (2017) 17046.
[18] M. Liu, X. Yin, E. Ulin-Avila, et al., Nature 474 (2011) 64.
[19] G.X. Ni, L. Wang, M.D. Goldflam, et al., Nat. Photon. 10 (2016) 244.
[20] D. Malko, C. Neiss, F. Viñes, et al., Phys. Rev. Lett. 108 (2012) 086804.
[21] X. Qin, Y. Liu, B. Chi, et al., Nanoscale 8 (2016) 15223–15232.
[22] G. Li, Y. Li, H. Liu, et al., Chem. Commun. 46 (2010) 3256–3258.
[23] Y. Li, L. Xu, H. Liu, et al., Chem. Soc. Rev. 43 (2014) 2572–2586.
[24] Z. Jia, Y. Li, Z. Zuo, et al., Acc. Chem. Res. 50 (2017) 2470–2478.
[25] C. Huang, Y. Li, N. Wang, et al., Chem. Rev. 118 (2018) 7744–7803.
[26] M. Long, L. Tang, D. Wang, et al., ACS Nano 5 (2011) 2593–2600.
[27] G. van Miert, V. Juričić, C. Morais Smith, Phys. Rev. B 90 (2014) 195414.
[28] H. Ren, H. Shao, L. Zhang, et al., Adv. Energy Mater. 5 (2015) 1500296.
[29] H. Tian, M.L. Chin, S. Najmaei, et al., Nano Res. 9 (2016) 1543–1560.
[30] Z. Jin, M. Yuan, H. Li, et al., Adv. Funct. Mater. 26 (2016) 5284–5289.
[31] C. Kuang, G. Tang, T. Jiu, et al., Nano Lett. 15 (2015) 2756–2762.
[32] J. He, N. Wang, Z. Cui, et al., Nat. Commun. 8 (2017) 1172.
[33] H. Du, H. Yang, C. Huang, et al., Nano Energy 22 (2016) 615–622.
[34] C. Lu, Y. Yang, J. Wang, et al., Nat. Commun. 9 (2018) 752.
[35] Y. Dong, Y. Zhao, Y. Chen, et al., J. Mater. Sci. 53 (2018) 8921–8932.
[36] Z. Zuo, D. Wang, J. Zhang, et al., Adv. Mater. 31 (2019) 1803762.
[37] M.M. Haley, S.C. Brand, J.J. Pak, Angew. Chem. Int. Ed. 36 (1997) 836–838.
[38] L. Wu, Y. Dong, J. Zhao, et al., Adv. Mater. 31 (2019) 1807981.
[39] J. Guo, R. Shi, R. Wang, et al., Laser Photonics Rev. (2020) 1900367.
[40] M. Sonoda, A. Inaba, K. Itahashi, et al., Org. Lett. 3 (2001) 2419–2421.
[41] R. Matsuoka, R. Sakamoto, K. Hoshiko, et al., J. Am. Chem. Soc. 139 (2017) 3145–3152.
[42] C. Huang, S. Zhang, H. Liu, et al., Nano Energy 11 (2015) 481–489.
[43] A.C. Ferrari, J.C. Meyer, V. Scardaci, et al., Phys. Rev. Lett. 97 (2006) 187401.
[44] X. Gao, J. Li, R. Du, et al., Adv. Mater. 29 (2016) 1605308.
[45] S.W. Cranford, D.B. Brommer, M.J. Buehler, Nanoscale 4 (2012) 7797–7809.
[46] M. Sheik-Bahae, A.A. Said, T. Wei, et al., IEEE J. Quantum Electron. 26 (1990) 760–769.
[47] R.A. Ganeev, A.I. Ryasnyansky, M. Baba, et al., Appl. Phys. B 78 (2004) 433–438.
[48] N. Dong, Y. Li, S. Zhang, et al., Opt. Lett. 41 (2016) 3936–3939.
[49] S. Kumar, M. Anija, N. Kamaraju, et al., Appl. Phys. Lett. 95 (2009) 191911.
[50] L. Kocsis, P. Herman, A. Eke, Phys. Med. Biol. 51 (2006) N91–N98.
[51] G. Demetriou, H.T. Bookey, F. Biancalana, et al., Opt. Express 24 (2016) 13033–13043.
[52] S. Lu, C. Zhao, Y. Zou, et al., Opt. Express 21 (2013) 2072–2082.
[53] X. Zheng, Y. Zhang, R. Chen, et al., Opt. Express 23 (2015) 15616–15623.
[54] X. Zheng, R. Chen, G. Shi, et al., Opt. Lett. 40 (2015) 3480–3483.
[55] J.P. Hermann, D. Ricard, J. Ducuing, Appl. Phys. Lett. 23 (1973) 178.
[56] P. Gaur, D. Sharma, N. Singh, et al., Spectrochim. Acta Part A: Mol. Biomol. Spectros. 97 (2012) 45–49.
[57] C.K. Sun, Y.L. Huang, S. Keller, et al., Phys. Rev. B 59 (1999) 13535–13538.
[58] B. Zhao, B. Cao, W. Zhou, et al., J. Phys. Chem. C 114 (2010) 12517–12523.
[59] J.E. Riggs, Y.P. Sun, J. Phys. Chem. A 103 (1999) 485–495.
[60] D.R. Lide, CRC Handbook of Chemistry and Physics, 85th ed., CRC Press, New York, 2004.